Contents lists available at ScienceDirect

# Virologica Sinica

journal homepage: www.keaipublishing.com/en/journals/virologica-sinica
www.virosin.org

Research Article

# Recombinant chimpanzee adenovirus vector vaccine expressing the spike protein provides effective and lasting protection against SARS-CoV-2 infection in mice

Mingqing Lu [a,b,c,1], Kunpeng Liu [b,c,1], Yun Peng [d,1], Zhe Ding [a,c,1], Yingwen Li [a,c], Alexander Tendu [a,c], Xue Hu [b], Ge Gao [d], Weiwei Guo [b,c], Hang Liu [d], Juhong Rao [b,c], Jiaxuan Zhao [b,c], Miaoyu Chen [d], Zhiming Yuan [d], Gary Wong [a,*], Chao Shan [b,*], Yanfeng Yao [d,*], Jiaming Lan [a,*]

[a] CAS Key Laboratory of Molecular Virology & Immunology, Institut Pasteur of Shanghai, Chinese Academy of Sciences, Shanghai, 200031, China
[b] State Key Laboratory of Virology, Chinese Academy of Sciences, Wuhan, 430071, China
[c] University of Chinese Academy of Sciences, Beijing, 100049, China
[d] Center for Biosafety Mega-Science, Wuhan Institute of Virology, Chinese Academy of Sciences, Wuhan, 430071, China

## ARTICLE INFO

## ABSTRACT

SARS-CoV-2 infection is a global public health threat. Vaccines are considered amongst the most important tools to control the SARS-CoV-2 pandemic. As expected, deaths from SARS-CoV-2 infection have dropped dramatically with widespread vaccination. However, there are concerns over the duration of vaccine-induced protection, as well as their effectiveness against emerging variants of concern. Here, we constructed a recombinant chimpanzee adenovirus vectored vaccine expressing the full-length spike of SARS-CoV-2 (AdC68-S). Rapid and high levels of humoral and cellular immune responses were observed after immunization of C57BL/6J mice with one or two doses of AdC68-S. Notably, neutralizing antibodies were observed up to at least six months after vaccination, without substantial decline. Single or double doses AdC68-S immunization resulted in lower viral loads in lungs of mice against SARS-CoV-2 challenge both in the short term (21 days) and long-term (6 months). Histopathological examination of AdC68-S immunized mice lungs showed mild histological abnormalities after SARS-CoV-2 infection. Taken together, this study demonstrates the efficacy and durability of the AdC68-S vaccine and constitutes a promising candidate for clinical evaluation.

## 1. Introduction

Severe Acute Respiratory Syndrome Coronavirus 2 (SARS-CoV-2), the causative agent of coronavirus disease 2019 (COVID-19), has caused a pandemic that shows no signs of abating (Zhu et al., 2020b). Unlike most other viral diseases, whose outbreaks were more limited in geographical scope, e.g., Ebola virus disease outbreaks/epidemics in Central/Western Africa, or Middle East respiratory syndrome (MERS) in the Middle East and the Western Asia, high numbers of COVID-19 cases have been continuously reported on all inhabited continents. According to the Coronavirus Resource Center at Johns Hopkins University, 519,936,669 confirmed cases and 6,259,865 deaths resulting from COVID-19 have been reported globally as of May 13, 2022 (JHU, 2021). A number of

vaccines were developed in response to this pandemic, with at least 14 different COVID-19 vaccines approved by the WHO for Emergency Use (WHO, 2021a). In addition, an estimated 156 different vaccines are currently under clinical development, and a further 198 ones are in the pre-clinical pipeline (WHO, 2021b).

In addition to mRNA vaccines, recombinant protein vaccines, inactivated vaccines, and viral-vectored vaccines have also been approved for emergency use. Among these, adenovirus (Ad)-vectored vaccines have substantial advantages including a strong safety record, and the ability to drive strong expression of the inserted gene due to the broad tissue tropism of Ad (Kerstetter et al., 2021). In addition, Ad can be readily scaled up via good manufacturing practice (GMP) production processes, enabling them to meet the global demand for SARS-CoV-2 vaccines, as

evidenced with the development of ChAdOx-vectored vaccines (Mendonça et al., 2021). Considering the influence of pre-existing immunity in humans (Elkashif et al., 2021), this class of vaccines typically use serotypes known to be rare in the human population (Bos et al., 2020), or adenovirus vectors from animal origin, including chimpanzee (van Doremalen et al., 2020) and gorilla (Capone et al., 2021) adenoviruses as vectors against SARS-CoV-2 infection.

At present, much of the global population has received between one and three doses of vaccine against SARS-CoV-2 (JHU, 2021), which has resulted in fewer COVID-19 related deaths. The attention now turns to whether vaccination can induce long-term sustained protection, and whether these vaccines are also protective against emerging variants of concern (VOC). In this study, we constructed a chimpanzee recombinant adenovirus vectored vaccine (AdC68-S) containing the SARS-CoV-2 spike (S) protein. After mice were immunized with either one or two doses of this vaccine, the immune responses induced by AdC68-S *in vivo* and their ability to protect against SARS-CoV-2 challenge were investigated.

## 2. Materials and methods

### 2.1. Cells and virus

HEK293T (ATCC: ACS-4500), HEK293 (ATCC: CRL-1573) and Vero E6 (ATCC: CRL 1586) cells were cultured in DMEM containing 10% Fetal bovine serum (FBS) at 37 °C in 5% $CO_2$. The SARS-CoV-2 isolate (nCoV-2019BetaCoV/Wuhan/WIV04/2019) employed in the challenge studies was obtained from the National Virus Resource, Wuhan Institute of Virology, Chinese Academy of Sciences. The recombinant virus rAd5-hACE2 was constructed, rescued, amplified and purified in-house (Xu et al., 2021).

### 2.2. Construction, rescue, amplification and purification of recombinant chimpanzee adenovirus vector vaccine AdC68-S

The codon optimized full-length *S* gene of SARS-CoV-2 (GenBank accession number MN908947.3) was synthesized by GenScript (Nanjing, China) and cloned into a pShuttle2 vector between the restriction sites *Not*I and *Kpn*I using restriction enzymes (NEB, USA). Subsequently, after digestion with *I-Ceu*I and *PI-Sce*I restriction enzymes, the whole S expression cassette containing the CMV promoter, *S* gene, and BGH polyA tail was inserted into the E1-deleted region of the chimpanzee adenoviral vector pAdC68 to generate the recombinant pAdC68-S. The empty chimpanzee adenovirus vector pAdC68 was utilized as the control. After linearization with *Pac*I, the recombinant pAdC68-S was transfected into HEK293 cells to generate recombinant AdC68-S. Following rescue, the recombinant virus was amplified in HEK293 cells and purified using cesium chloride density gradient ultracentrifugation. The viral particle titer was determined spectrophotometrically and the vaccine stocks were stored at −80 °C.

### 2.3. Western-blot identification of recombinant virus AdC68-S

HEK293 cells in 6-well plates were infected with AdC68-S and empty AdC68 at a dose of $10^9$ viral particles (vp) per well. At 24 h after infection, the cells were harvested in RIPA lysis buffer with a proteinase inhibitor of phenylmethylsulfonyl fluoridenone (PMSF), the protein samples were separated by SDS-PAGE and transferred to a PVDF membrane at 150 V for 70 min. The membranes were then incubated with a primary antibody against the SARS-CoV-2 S protein (No.40150-T62-CoV2, Sino Biological, China), following incubation with HRP-conjugated goat anti-rabbit secondary antibodies (A0208, Beyotime Biological, China). The expression of GAPDH was used as an internal control. The membrane was visualized using Chemister™ High-sig ECL Western Blotting Substrate (No.180-501, Tanon, China).

### 2.4. Animals, immunization, challenge, and sample collection

Forty-four female, 6–8 weeks old, wild-type C57BL/6J mice were purchased from Beijing Vital River Laboratory Animal Technology Co., Ltd and divided into six groups (3 different immunogens, 1 or 2 vaccine doses) for the detection of immune responses and long-term challenge studies. The PBS and AdC68 control groups each contained 12 mice. The AdC68-S experiment group included 20 mice. Twenty-two female, 6–8 weeks old, transgenic hACE2 mice were purchased from GemPharmatech Co., Ltd. and divided into six groups (the same as the wild-type C57BL/6J mice groups) for short-term challenge studies. The PBS and AdC68 control groups each contained six animals. The two AdC68-S experiment groups included five mice each.

For immunization, the wild-type and transgenic C57BL/6J mice were injected intramuscularly with 50 μL PBS, or an equal volume containing $1 \times 10^{11}$ vp of recombinant AdC68 or AdC68-S once (1 dose), or twice (2 doses) at a 21-day interval. For wild-type C57BL/6J mice, 3 mice in each group were sacrificed (except for 5 mice in the two-dose AdC68-S group). Sera and splenocytes were harvested for detection of humoral and cellular immune responses. For all groups, sera were also harvested at 4 months (day 141) and 6 months (day 201) after the last immunization. At the 6-month timepoint, the mice received an intranasal challenge of $1 \times 10^5$ $TCID_{50}$ SARS-CoV-2 in 50 μL PBS. For wild-type C57BL/6J mice, they also received an intranasal administration of $1 \times 10^{10}$ vp rAd5-hACE2, which render the mice transiently susceptible to SARS-CoV-2 infection (Xu et al., 2021). For the transgenic mice, the animals received $1 \times 10^5$ $TCID_{50}$ SARS-CoV-2 in 50 μL PBS, administered intranasally at 21 days after the last immunization. At 5 days after challenge, the lung tissues were harvested for viral load determination via PCR and live virus titration, as well as pathology assessment.

### 2.5. Antibody detection by enzyme-linked immunosorbent assay (ELISA)

96-well microplates were coated with recombinant SARS-CoV-2 S protein (CG-202-01, Vazyme, China) at a concentration of 50 ng per well. After incubation at 4 °C overnight, the plates were washed and blocked with 5% non-fat dry milk. A total volume of 100 μL mice sera were serially diluted 2-fold, starting at 1:25, in PBS supplemented with 5% non-fat dry milk, and added to each well. After incubation at 37 °C for 2 h, diluted HRP-conjugated goat anti-mouse IgM (1:10000), IgG, IgG1 or IgG2a (1:3000 each) were added. Following 1.5 h incubation at 37 °C with TMB (Beyotime, China), the plate was washed and the reaction was stopped by 2 mol/L $H_2SO_4$. The OD values at 450 nm were then measured by using the ELISA microplate reader.

### 2.6. Neutralizing antibody detection by pseudovirus neutralization assay

Levels of neutralizing antibodies in the immunized mouse sera were determined using a SARS-CoV-2 pseudovirus system based on a lentivirus (HIV-1) backbone. In brief, the pseudovirus was generated by co-transfection of HEK293T cells with the HIV backbone expressing firefly luciferase (pNL4-3.Luc.R-E-) and pVAX1 encoding S proteins from the wild type S protein Wuhan-Hu-1 (GenBank: MN908947.3), the Alpha variant (GenBank: MW422255), the Gamma variant (GenBank: MW869183), the Delta variant (GenBank: MW989805), the Epsilon variant (GenBank: MW550155), the Omicron variant (GenBank: OM172026). After 48 h, the cell supernatant containing the pseudovirus was collected, measured, and stored at −80 °C until further use. Serum samples were serially diluted 2-fold in 96-well tissue culture plates, and incubated at 37 °C for 2 h after the addition of SARS-CoV-2 pseudovirus to each well. The resultant mixtures were then transferred to duplicate wells containing confluent Huh7.5.1 cells. After incubation for 72 h, the luciferase assay was performed using an Ultra 384 luminometer (Tecan, Switzerland). The amount of neutralizing antibodies was calculated as: (Relative luciferase units of mock sera – relative luciferase units of immune serum for a given dilution)/Relative luciferase units of mock sera.

## 2.7. Plaque reduction neutralization test (PRNT) of SARS-CoV-2

Vero E6 cells were seeded in a 24-well plate with $1 \times 10^5$ cells/well overnight. The next day, sera from mice were serially diluted in DMEM and incubated with 100 $TCID_{50}$ SARS-CoV-2 at 37 °C for 1 h. DMEM without sera was used as a negative control. The mixture was then added to the Vero E6 cells. After incubation at 37 °C for 1 h, the supernatants were completely removed, the cells were washed with PBS, and replaced with 0.9% methylcellulose-2% FBS-DMEM. Plaque formation was observed daily in the infected Vero E6 cells. Four days later, the overlay was removed, and the cells were fixed with 4% paraformaldehyde and stained with 0.1% crystal violet solution. The plaques from serum-treated wells were normalized to those of non-treatment controls (set as 100%). The dilution of sera which reduced the percentage of plaques by 50% ($PRNT_{50}$) was calculated using nonlinear regression analysis.

## 2.8. Evaluation of antigen-specific T-cell responses by enzyme-linked immunospot (ELISpot) assay

An IFN-γ ELISpot assay was performed following manufacturer instructions (3321-4APT-10, Mabtech, Sweden) to evaluate the antigen-specific T-cell responses induced by the AdC68-S vaccine. In brief, freshly harvested splenocytes ($5 \times 10^5$/well) were stimulated in duplicate for 24 h with 4 mg/mL of a synthesized 18-mer peptide library (GenScript, China) spanning the entire S protein of SARS-CoV-2, with overlaps of 10 amino acids. After 20–24 h of stimulation, biotinylated detection antibody and streptavidin-horseradish peroxidase were added. The numbers of IFN-γ spot-forming cells (SFCs) were counted after the addition of 3-amino-9-ethylcarbazole (AEC) substrate solution. Phorbol 12-myristate 13-acetate (PMA) was added to the positive-control group, whereas the negative-control group received no stimuli. The numbers of antigen-specific IFN-γ secreting T-cells were calculated by Smart-count in the Cellular Technology Limited (CTL) software.

## 2.9. Viral load detection by real time quantitative reverse transcriptase PCR

After the mice were euthanized, the lungs were collected for viral load examination. The right lung was homogenized in 1 mL DMEM in a tissue grinder. One hundred and forty μL of the homogenate was then subjected to RNA isolation using the Qiagen RNeasy Mini kit (74104, Qiagen, China), and the total RNA was eluted in 50 μL RNase-free water. cDNA was synthesized from 3 μL total RNA in a 20 μL reaction system using the PrimeScript™ RT reagent Kit with gDNA Eraser (RR047A, Takara, Japan). Viral copies were quantified from 1 μL cDNA template by standard curve method on the ABI 7500 (using the Takara TB Green® Premix Ex Taq™ II) with a pair of primers targeting the *S* gene: forward primer 5'-CAATGGTTTAACAGGCACAGG-3'; reverse primer 5'-CTCAAGTGTCTGTGGATCACG-3'. The standard curve was constructed with the following viral copies in a 20 μL reaction system ($2.35 \times 10^9$ copies, $2.35 \times 10^8$ copies, $2.35 \times 10^7$ copies, $2.35 \times 10^6$ copies, $2.35 \times 10^5$ copies, $2.35 \times 10^4$ copies, $2.35 \times 10^3$ copies, $2.35 \times 10^2$ copies). Samples $<2.35 \times 10^2$ copies were defined as negative. The copy numbers for positive samples were calculated with the equation: (sample well - blank well) copies $\times$ 20 $\times$ 10/0.2 mL/g lung tissue in 1 mL.

## 2.10. Viral isolation from the lungs of challenged mice

Fifty μL of the lung tissue homogenate was used in a 10-fold gradient dilution ($10^{-1}$, $10^{-2}$, $10^{-3}$, $10^{-4}$, $10^{-5}$, $10^{-6}$), and 150 μL of each dilution was inoculated onto a monolayer of Vero E6 cells seeded in 24-well plates for 1 h. Afterwards, the inoculum was completely removed. The cells were washed once with PBS and then overlaid with 0.9% methylcellulose-2% FBS-DMEM. Four days later, the covering was removed and the cells were fixed with 4% paraformaldehyde and stained with 1% crystal violet solution. The plaques were manually counted and the viral

titer was calculated, in which no plaques at the $10^{-1}$ dilution were defined as negative. The limit of the plaque assay experiments was approximately 67 PFU/mL.

## 2.11. Histopathology detection from the lungs of challenged mice

The left lung was used for histopathology detection. Samples were fixed in 10% neutral buffered formalin, embedded in paraffin, sequentially sectioned to 4-μm thickness, and stained with haematoxylin and eosin (HE) prior to examination by light microscopy. To obtain a representative result, different sites of the lung tissue were sampled for the histopathology analysis. Finally, quantitation of 4–5 slides per animal was used to assess the overall effect and the impact of vaccination on the challenged animals.

## 2.12. Statistical analysis

Statistical analyses were conducted using one-way ANOVA with Bonferroni post-test via SPSS. The unpaired two-tailed Student's *t*-test was used to compare means between different groups. A value of $P < 0.05$ was taken to indicate statistical significance. Results were expressed as mean $\pm$ SD. All figures were generated using the Prism 5 software package.

## 3. Results

### 3.1. Successful rescue of the recombinant chimpanzee adenovirus expressing the full SARS-CoV-2 S protein

To acquire the recombinant AdC68-S vaccine, the recombinant pAdC-68-S was constructed as Fig. 1A. The linearized plasmid pAdC68-S was transfected into HEK293 cells. Cytopathic effects (CPE) including cellular enlargement, rounding and detachment from the wall of the culture flask were observed 10 days after the transfection (Fig. 1B). When the CPE was present in over 90% of the monolayer, the cells were harvested and expression of the S protein was assayed by Western-blot. As shown in Fig. 1C, the S protein, approximately 200 kDa in size, was observed in the PVDF membrane. After large scale amplification and purification, the harvested virus titer was $2.86 \times 10^{12}$ vp/mL. The control empty vector AdC68 titer was determined to be $1.94 \times 10^{12}$ vp/mL using the same methods.

### 3.2. AdC68-S induced rapid and robust humoral and cellular immune responses in mice after one or two doses

The immunization and challenge schedules of wild-type and transgenic mice were shown in Fig. 2A and Fig. 2B respectively. AdC68-S was administered to the mice in one dose ($1 \times 10^{11}$ vp) or two doses at a 21-day interval. Seven days after each immunization, the sera and splenocytes were harvested for the detection of specific humoral and cellular responses. As shown in Fig. 3A, AdC68-S induced a high level of cellular immune responses. Additionally, two doses of vaccination induced a significant T-cell response compared to the one dose vaccination group ($P < 0.01$), as evidenced by a higher frequency of IFN-γ secreting cells.

Seven days after the injection of AdC68-S, specific IgM and IgG could be detected in the sera of the immunized mice. Subsequently, after the second dose of AdC68-S, the IgG titer increased dramatically ($P < 0.001$) at 28 days after the first immunization (Fig. 3B). Further studies indicated that the high titer of IgG consisted of both IgG1 and IgG2a subtypes, indicating that AdC68-S induced a mixed Th1/Th2 immune response, but with a Th1 bias, as shown in Fig. 3C.

Furthermore, pseudovirus neutralization and $PRNT_{50}$ assays were conducted to analyze the level of neutralizing antibodies induced by AdC68-S. Seven days after injection of the first vaccine dose, neutralizing antibodies were detected in all three mice (AdC68-S1–S3 in Fig. 3D). Additionally, seven days after the second injection in the two-dose group,
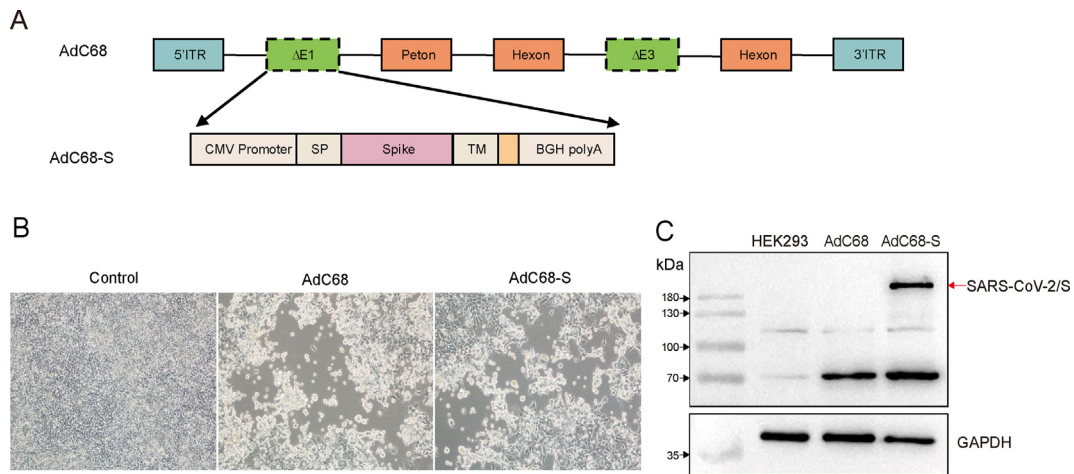
**Fig. 1.** Construction and confirmation of the AdC68-S vaccine candidate. **A** Schematic diagram of recombinant plasmid AdC68 construction. **B** Cytopathic effect (CPE) was observed in HEK293T cells transfected with linearized plasmids AdC68-S or AdC68. Magnification: ×200. **C** The S protein was detected in HEK293T cells infected with AdC68-S via Western blotting. GAPDH was used as the internal control.
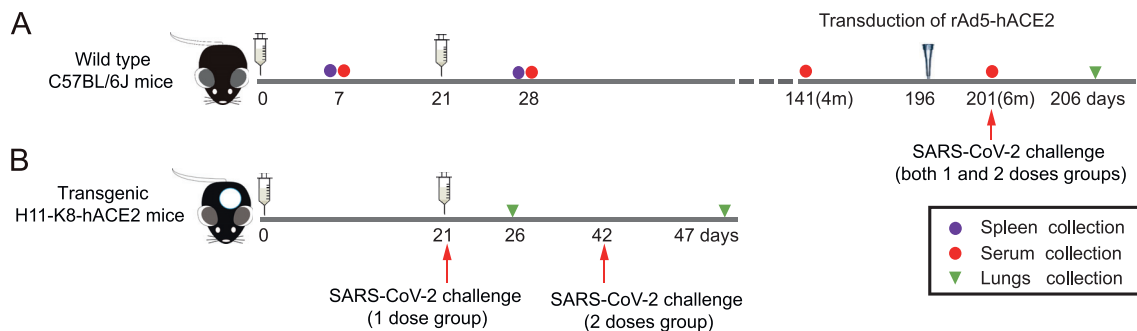


**Fig. 2.** Immunization and challenge schedule for mice. **A** Wild-type C57BL/6J mice were immunized with the recombinant vaccine either once (1 dose) or twice (2 doses). Seven days after each immunization, the sera and splenocytes were harvested for immune response detection. Four or six months after the last immunization in the two different dose group, the sera were harvested for antibody detection. In addition, both mouse groups were challenged with SARS-CoV-2 intranasally at six months after the second dose. The mice were transduced with rAd5-hACE2 five days before challenged with SARS-CoV-2. The lungs were harvested for detection of viral loads and live virus titers five days after the challenge. **B** Transgenic mice H11-K8-hACE2 were immunized with the same regimens. At twenty-one days after each immunization, the mice were challenged intranasally with SARS-CoV-2. Similarly, the lungs were harvested for the detection of viral loads and live virus titers at five days after the challenge.

a high level of neutralizing antibodies (50% Pseudovirus Inhibition ($PI_{50}$) as high as 980.98) was observed in all five mice (AdC68-S1–S5 in Fig. 3E). Levels of neutralizing antibodies detected in the pseudovirus neutralization assay were further quantified through a $PRNT_{50}$ assay using live SARS-CoV-2 (Isolate: nCoV-2019BetaCoV/Wuhan/WIV04/2019), which showed that the vaccine induced high level of neutralizing antibodies at seven days after each immunization (Fig. 3F). The $PRNT_{50}$ of the one and two-dose immunization groups were 321.37 and 1166, respectively. More importantly, the neutralizing antibodies, especially at higher antibody titers, are also able to neutralize several current representative divergent SARS-CoV-2 variants of concern, although the neutralization ability decreased 10–20 fold (Fig. 3G).

### 3.3. AdC68-S significantly reduced the viral load in lung tissues and protected mice against SARS-CoV-2 challenge in mice

To investigate the efficacy induced by the recombinant vaccine, the mice were challenged with SARS-CoV-2 at 21 days after the hACE2 transgenic mice were immunized with the recombinant AdC68-S (one or two doses). As shown in Fig. 4A, viral RNA in the lungs decreased dramatically in the AdC68-S group compared with the PBS or AdC68 control groups, especially after the mice received two doses of the vaccine. Similarly, live virus titers in the lungs of the vaccine immunized

mice were at undetectable levels, as shown in Fig. 4B. Consistently, there were fewest pathogenic changes observed in the SARS-CoV-2 infection in the AdC68-S group, as shown in Fig. 4C. The lungs in the AdC68-S vaccinated mice showed a slight proliferation of inflammatory cells around the blood vessels, mainly consisting of lymphocytes and monocytes (Fig. 4C, panels i and iv). In contrast to the AdC68-S vaccine group, the lungs of the mice in the AdC68 and PBS control groups showed widening of the interstitial space, inflammatory cell proliferation and other changes associated with interstitial pneumonia, as shown in Fig. 4C (panels ii, iii, v and vi). The panoramic scans of the lungs were shown in Supplementary Fig. S1.

### 3.4. AdC68-S induced long-lasting antibodies response in mice

To characterize long-term immune responses induced by either vaccination regimens, the sera of the mice were collected at four and six months after the last immunization and the total IgG and neutralizing antibodies were assayed. As shown in Fig. 5A, in both vaccine immunization regimens, the total S-specific IgG remained at high levels and did not show a significant decline even at six months post-vaccination. Pseudovirus neutralization assay results showed that neutralizing antibodies could still be detected in most (75%–100%) of the immunized mice, as shown in Fig. 5B, C, E and F. The $PI_{50}$ values of one and two dose
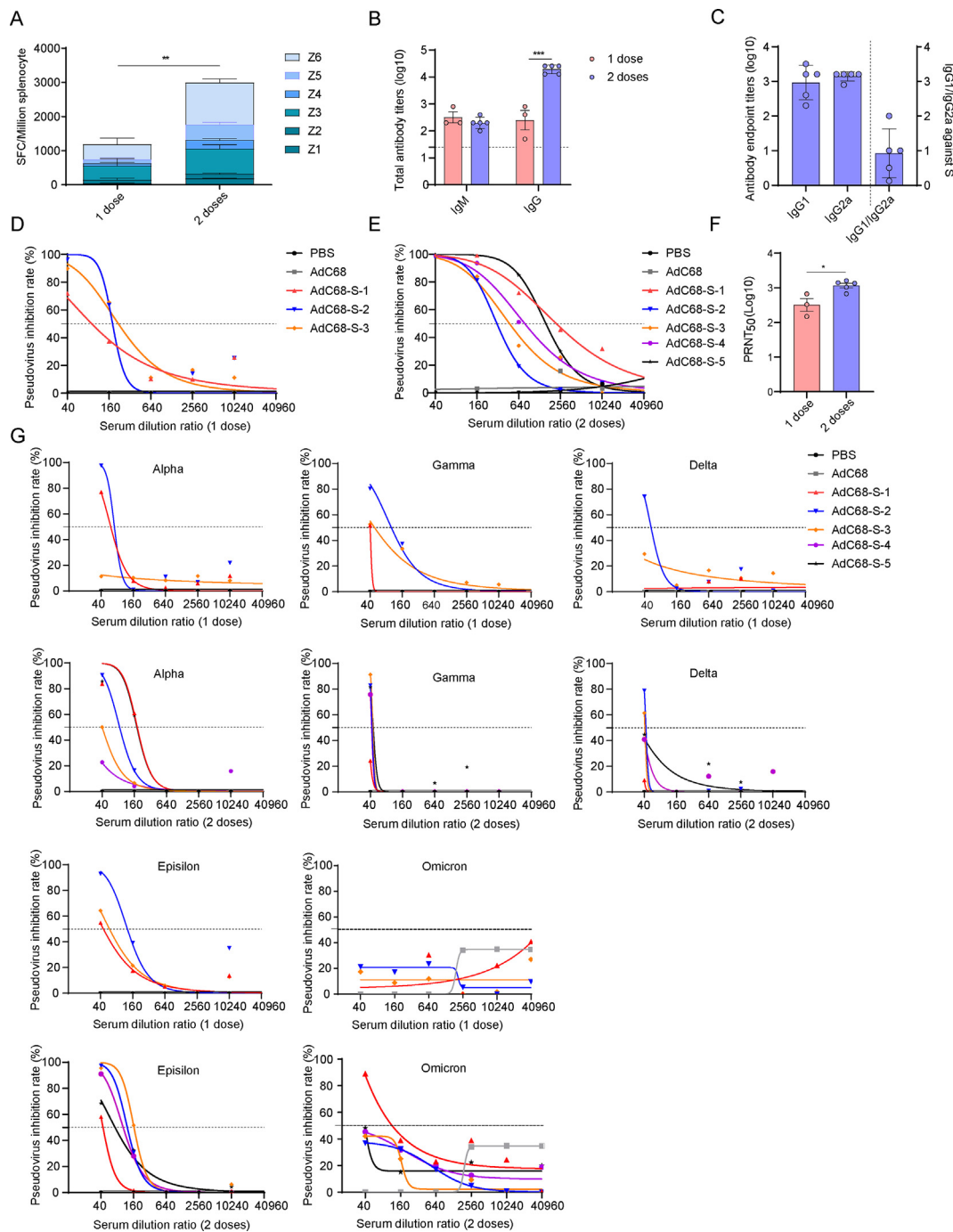
**Fig. 3.** Immune responses induced by AdC68-S in mice. **A** IFN-γ secreting splenocytes induced by the vaccine were detected by ELISpot in wild-type C57BL/6J mice at 7 days after the first or second immunization. Z1-Z6 indicate different peptide pools covering full length of the S protein. **B** Binding antibodies from mice sera at 7 days after the first or second immunization were detected by ELISA. **C** Antibody subtyping of IgG1 and IgG2a in the mice sera at 7 days after the second immunization. **D–E** Neutralization test of SARS-CoV-2 pseudovirus at 7 days after one dose (**D**) and two dose immunization (**E**). **F** Neutralizing antibody detection based on live SARS-CoV-2 at 7 days after the first or second immunization. **G** Neutralization of different SARS-CoV-2 variant pseudoviruses at 7 days after 1 dose (top row) and 2 dose (below row) immunization. Different variants of SARS-CoV-2 include Alpha, Gamma, Delta, Epsilon and Omicron. The vaccine had the best neutralization ability against the Alpha and Epsilon variants, followed by the Gamma and Delta variants, and the neutralization to Omicron variant was the least effective.

groups at four months, and the one and two-dose groups at six months were 447.16, 223.35, 992.09, and 478.93, respectively. The neutralizing antibody titers as detected by PRNT against live SARS-CoV-2 were found to be over 1:1000 (Fig. 5D) in all of the vaccine immunized groups, including the single and dual dose groups, at four and six months after the last immunization. Additionally, the vaccine induced long-lasting neutralizing antibodies against current representative SARS-CoV-2 variants of concern four months after the immunization, but the vaccine has

the least neutralization observed with delta and omicron variants, as shown in Fig. 5G. When it came to the six months after the immunization, long-lasting neutralizing antibodies had the highest neutralization ability against the Alpha variants and the least neutralization ability against the Delta variants in Supplementary Fig. S2 (the neutralization ability to the Omicron variants was not detected due to sera limitations). Overall, one and two doses immunization with AdC68-S induced long-term antibody responses in mice lasting at least 6 months.
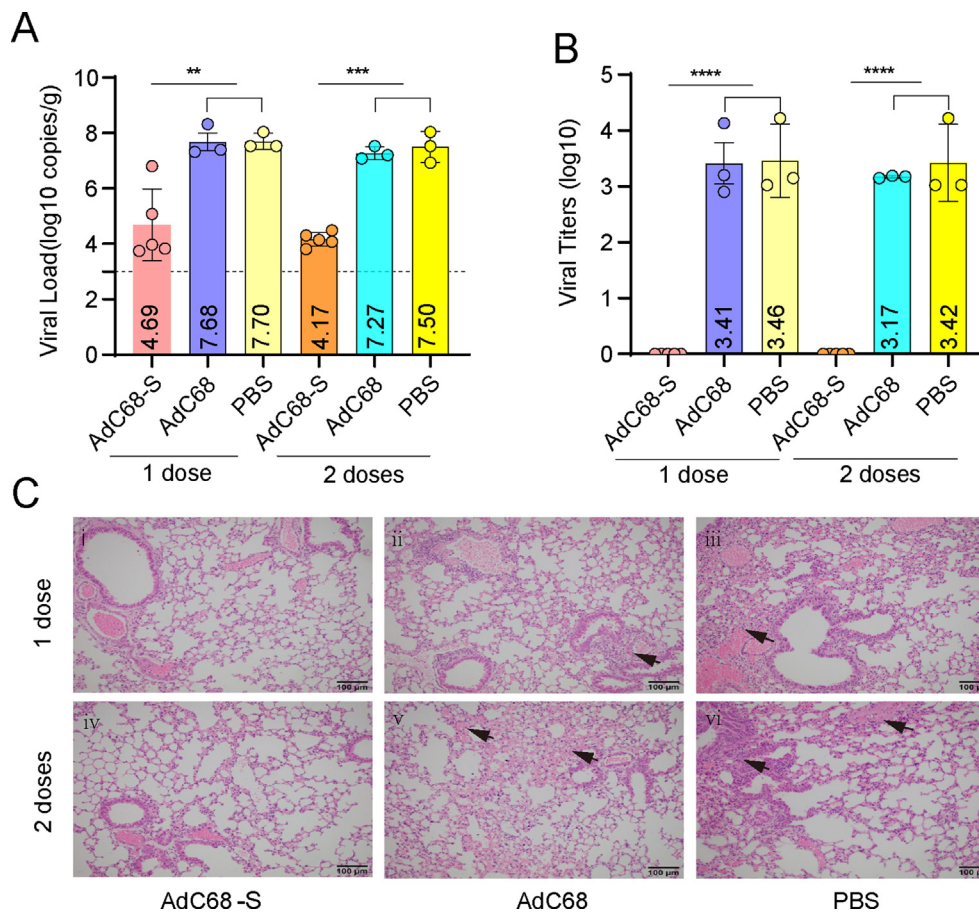
**Fig. 4.** Viral load and live virus titers in hACE2 transgenic mice challenged with SARS-CoV-2. **A** Viral load in the lungs of mice. **B** Live viral titers in the lungs of mice. **C** Histopathology results for the lung tissues of mice. Panels i-iii (top row) represent lung samples after 1 immunization dose. Panels iv-vi (below row) represent lung samples after 2 immunization doses.

*3.5. AdC68-S provides long-term protection against SARS-CoV-2 infection in mice*

Six months after the second immunization with AdC68-S, all wild-type C57BL/6J mice were transduced with recombinant Ad5-hACE2 and challenged with SARS-CoV-2 five days later. The lungs were then harvested at five days after the challenge. In Fig. 6A, the vaccine was observed to decrease the viral load to undetectable levels. Consistently, SARS-CoV-2 could not be detected in the lungs of the immunized mice (Fig. 6B). The effective protection by the vaccine was verified by pathological changes in the lung tissues. In Fig. 6C (panels i and iv), the mice in the immunized groups showed mild histological abnormalities, and slight atrophy of the local alveoli. Conversely, the mice in the AdC68 or PBS immunized groups (Fig. 6C, panels ii, iii, v and vi) showed severe abnormal tissue structure and parenchyma involving a large area of the lungs. Furthermore, a small number of epithelial cells were shed in the bronchus and a large number of inflammatory cells could be observed in the tissue. The panoramic scans of the lungs were shown in Supplementary Fig. S3.

**4. Discussion**

Over two years have passed since the start of the COVID-19 pandemic, with the end nowhere in sight. Although many vaccines including those based on the inactivated virus (Palacios et al., 2020; Wang et al., 2020), mRNA (Polack et al., 2020; Laczkó et al., 2020), viral-vector (Zhu et al., 2020a; Logunov et al., 2021), and recombinant protein (Keech et al., 2020; Yang et al., 2020; Heath et al., 2021) have been widely administered to the human populations, many questions are yet to be

conclusively answered. It is unknown whether current vaccines, especially those based on delivery of the S protein, are able to provide long-term protection, and whether this strategy is also effective against emerging SARS-CoV-2 variants of concern. In this study, we investigated these questions by testing the candidate vaccine AdC68-S in a mouse model.

SARS-CoV-2 is mainly transmitted through droplets from the cough, sneeze or breath of an infected person (Scheuch, 2020). Additionally, these droplets may contaminate food and other objects in the surrounding environment (Ong et al., 2020), and possibly infect humans via fomites. A rapid and highly effective COVID-19 vaccine with long lasting protection would be of vital importance in combating the COVID-19 pandemic. The results from this study show that at seven days after intramuscular administration of AdC68-S, both IgM and IgG antibodies were detected. Several previously published studies (Tostanoski et al., 2020; Khoury et al., 2021; McMahan et al., 2021) have suggested that neutralizing antibodies could serve as a correlate of protection induced by vaccination against SARS-CoV-2 infection. Thus, we characterized the neutralizing activity of vaccine-induced antibodies by pseudovirus and live SARS-CoV-2 neutralization assays. Effective induction of cellular immune responses was also evidenced by IFN-γ secreting splenocytes at seven days after administration of the AdC68-S vaccine. The protective efficacy of a single dose of the vaccine was also demonstrated in the hACE2 transgenic mouse challenge model. Consistent with our results, an AdC68-19S (Li et al., 2021b) study conducted by another group showed that the vaccine could induce specific immune responses and protect animals against SARS-CoV-2 infection. The rapid immune response elicited by the vaccine candidate described in this study further reinforces these findings and supports the feasibility of using AdC68-vectored
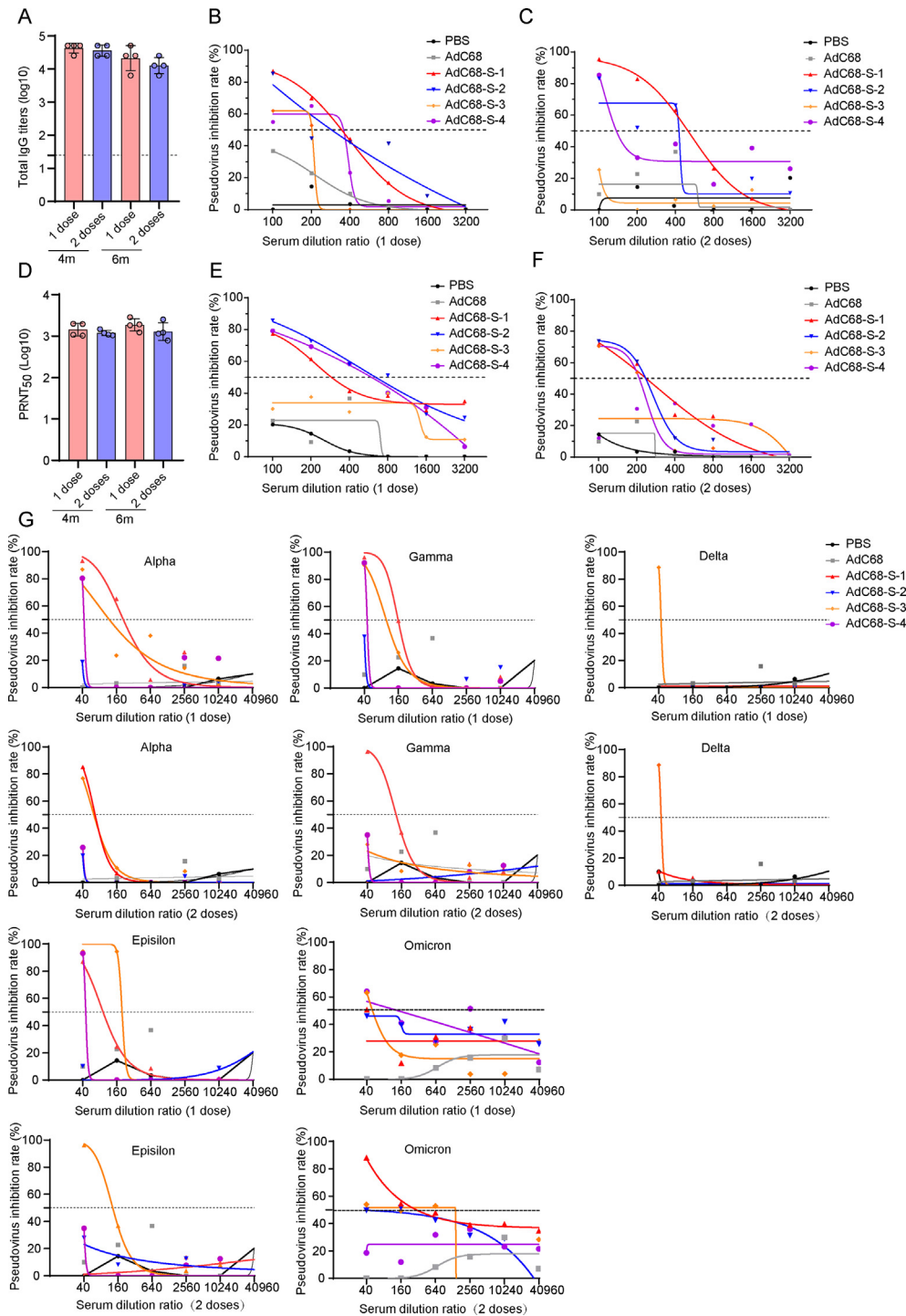
**Fig. 5.** Long-term immunization responses induced by AdC68-S in mice. **A** IgG binding antibodies of mice immunized with one or two doses AdC68-S were detected after four or six months by ELISA. **B–C** The pseudovirus neutralization of SARS-CoV-2 was tested at 4 months after one (**B**) and two-dose (**C**) immunization. **D** Neutralization antibodies of mice immunized with one or two doses AdC68-S after four or six months by live SARS-CoV-2 (WIV04). **E–F** The pseudovirus neutralization of SARS-CoV-2 was tested at 6 months after one (**E**) and two-dose (**F**) immunization. **G** Neutralization of different SARS-CoV-2 variant pseudovirus at 4 months after one dose (top line) and two doses (below line) immunization. Different variants of SARS-CoV-2 include Alpha, Gamma, Delta, Epsilon and Omicron respectively. The vaccine had neutralization ability against the Alpha, Gamma, Delta and Epsilon variants.

vaccines for emergency immunization of medical personnel, who are at high risk of exposure to the SARS-CoV-2.

Pre-existing immunity to adenoviral vectors, which may result in the reduction of efficacy and unwanted side effects, is one of the most criticized shortcomings for this class of viral-vectored vaccines (Elkashif et al., 2021). We therefore utilized a chimpanzee adenovirus as the backbone for this vaccine candidate, in which the vector is known to have low seroprevalence rates in the human population. A second concern with adenovirus vaccines is whether the candidate could be applied as a homologous prime-boost regimen. Our results showed that at
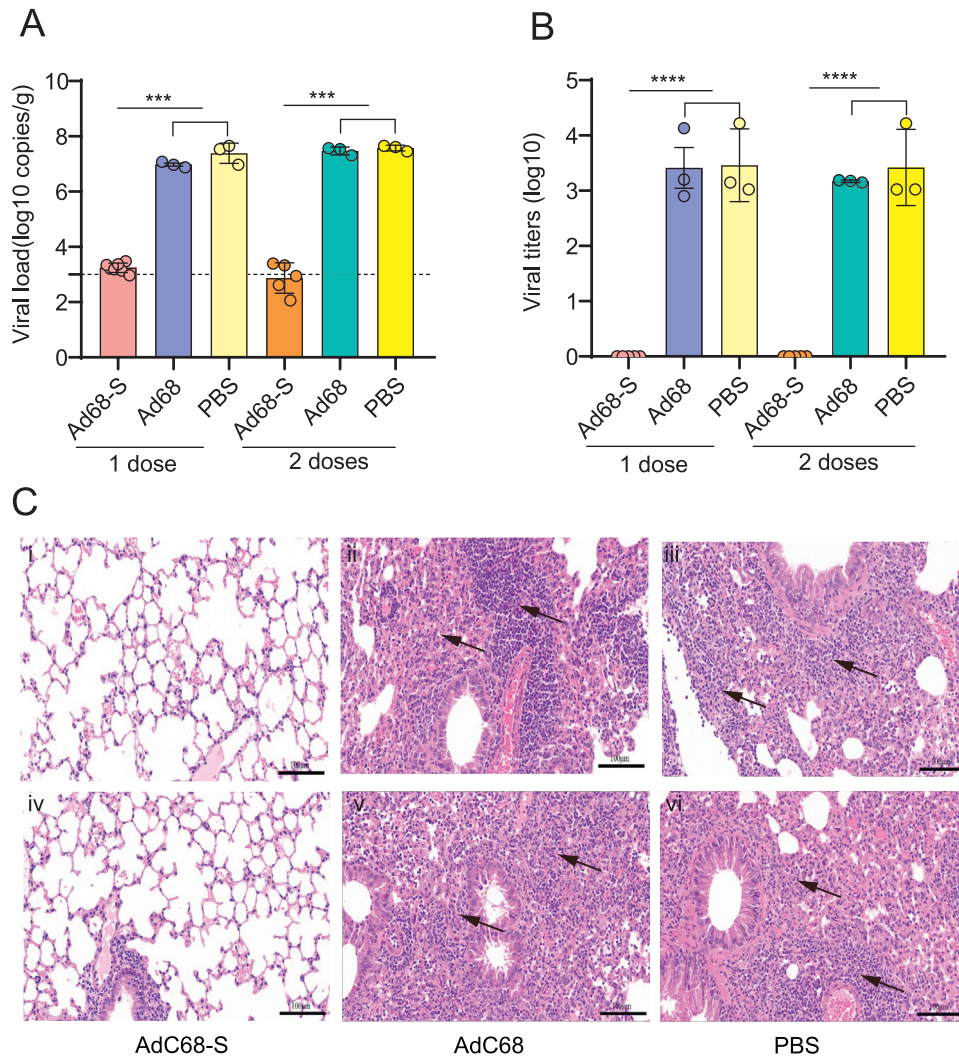
**Fig. 6.** Viral load and live virus titers of wild-type C57BL/6J mice challenged with SARS-CoV-2. The mice were transduced with rAd5-hACE2 before virus challenge. Viral load (**A**) and live virus titers (**B**) in lungs tissues of mice. **C** Histopathology results for the mouse lung tissue. Panels i-iii (top row) represent lungs samples after one dose immunization. Panels iv-vi (below row) represent lungs samples after two dose immunization.

seven days after the boost immunization, higher levels of Th1 and Th2 antibody responses, neutralizing antibodies and cellular immune response were detected, compared to animals that only received one dose. However, since the sera and splenocytes of mice immunized with a single dose were not analyzed at the same time (28 days after one shot immunization) as the mice receiving the two dose regimens, it cannot be concluded whether an enhanced level of humoral and cellular immune responses was induced by the second immunization, or the residual response to the initial vaccine prime. This will be a topic of future investigations. Regardless, the *in vivo* experiments indicated that one dose of the AdC68-S vaccine was sufficient for protection, and that in this mouse challenge model, a second dose was not needed for further protection.

The duration of vaccine-induced antibody responses is also recurring, unresolved question regarding current COVID-19 vaccine candidates. Although a previous AdC68-19S study showed that sustained antibody responses can be induced in mice (Li et al., 2021b), long-term protection was not verified by SARS-CoV-2 challenge. In this study, we observed vaccine-induced neutralizing antibodies at four and six months after the last immunization, and antibody levels were high for both the single-dose and two-dose groups. Neutralization assays with live SARS-CoV-2 showed that the antibody titers were over 1:1000, but the results generated with the pseudovirus assay showed large within-group

differences, especially in the 2 doses group at the 4-month timepoint (Fig. 5C). We believe that the pseudovirus neutralization assay system, rather than the vaccination itself, resulted in this difference as the same sera showed excellent within-group neutralization consistency (Fig. 5D) with SARS-CoV-2 live virus. AdC68-S conferred complete protection against SARS-CoV-2 challenge at six months after immunization in a mouse model pre-transduced with rAd5-hACE2. The specific role of memory T- or B-lymphocytes in maintaining the observed long-term immunity remains to be elucidated, and will be part of our future investigations.

In this study, hACE2 transgenic mice and wild-type mice pre-transduced with rAd5-hACE2 were utilized in experiments to characterize the short-term and long-term protection, respectively, against SARS-CoV-2. This was based on the previously-reported effects of aging in mice, which may also impact susceptibility to SARS-CoV-2 infections. With increasing age and decline in immune function, mice often develop spontaneous tumors and other age-related complications, which may be more prominent in transgenic mice models. In order to mitigate these potentially confounding factors, we selected the most representative transgenic mouse model for short-term protection studies, while wild-type mice were selected for long-term investigations. Both animal models were shown to be useful for studying SARS-CoV-2 infection (Bao et al., 2020; Sun et al., 2020a; Sun et al., 2020b) and have been widely

used in the development of specific vaccines (Ma et al., 2020; Huang et al., 2021), antibodies (Hassan et al., 2020; Li et al., 2020; Ge et al., 2021) and therapeutic agents (Li et al., 2021a). In a previous study, scientists (Rathnasinghe et al., 2020) compared these two mice models, and demonstrated that the K18-hACE2 model provides a stringent model for testing vaccines and antivirals, whereas the adenovirus transduction model could be used across multiple genetic backgrounds and modified mouse strains to study SARS-CoV-2 infections.

## 5. Conclusions

With the emergence of VOCs and specific variants of interest (VOIs), all SARS-CoV-2 vaccine candidates face the potential challenge of reduced protection towards these VOCs and VOIs. In this study, the sera of mice immunized with AdC68-S were tested for neutralization against different variants of SARS-CoV-2 via a pseudovirus neutralization assay. The results showed that the sera could neutralize selected variants with good levels of neutralization against the alpha VOC, but poor levels of neutralization against the delta VOC. This result is consistent with a previous study using sera from convalescent patients in Wuhan (Liu et al., 2021). In addition, the pseudovirus neutralization assay showed that the sera of mice with higher titers of neutralizing antibodies against the parent strain were more likely to neutralize the other variants of SARS-CoV-2, which may be due to the induction of broad-spectrum antibodies. Further investigation into the nature and mechanism of action for this array of neutralizing antibodies may contribute to the development of broad-spectrum vaccines and immunotherapeutics against SARS-related coronaviruses in the future.

## Data availability

The original contributions presented in the study are included in the article/supplementary material, further inquiries can be directed to the corresponding author/s.

## Ethics statement

The animal experiments were approved by the Animal Ethics Committee at the Wuhan Institute of Virology, Chinese Academy of Sciences (approval number: WIVA21202009). The experiments involving SARS-CoV-2 were performed in the Biosafety Level 3 (BSL-3) laboratory in the Center for Biosafety Mega-Science, Wuhan Institute of Virology, Chinese Academy of Sciences, and approved by the Biosafety Committee of the Wuhan Institute of Virology, Chinese Academy of Sciences (approval number: NBL4C21010).

## Author contributions

Mingqing Lu: data curation, formal analysis, methodology, project administration, software, writing – original draft, writing – review and editing. Kunpeng Liu: data curation, formal analysis, investigation, methodology, project administration, validation. Yun Peng: methodology, project administration. Zhe Ding: data curation, formal analysis, methodology, project administration, writing – original draft. Yingwen Li: methodology, project administration, software. Alexander Tendu: project administration, writing – original draft. Xue Hu: project administration. Ge Gao: project administration. Weiwei Guo: project administration. Hang Liu: project administration. Juhong Rao: project administration. Jiaxuan Zhao: project administration. Miaoyu Chen: project administration. Zhiming Yuan: funding acquisition, resources, supervision. Gary Wong: conceptualization, funding acquisition, resources, writing – original draft, writing – review and editing. Chao Shan: Conceptualization, Funding acquisition, Resources, Supervision, validation, writing – review and editing. Yanfeng Yao: conceptualization, data curation, formal analysis, funding acquisition, methodology, project administration, resources, supervision, validation, visualization, writing – review and editing. Jiaming Lan: conceptualization, data curation, formal analysis, funding acquisition, project administration, resources, software, supervision, writing – original draft, writing – review and editing.

## Conflict of interest

The authors declare no conflict of interests.

## Acknowledgements

## Appendix A. Supplementary data

Supplementary data to this article can be found online at https://doi.org/10.1016/j.virs.2022.05.006.

## References

Bao, L., Deng, W., Huang, B., Gao, H., Liu, J., Ren, L., Wei, Q., Yu, P., Xu, Y., Qi, F., 2020. The pathogenicity of SARS-CoV-2 in hACE2 transgenic mice. Nature 583, 830–833.

Bos, R., Rutten, L., van der Lubbe, J.E., Bakkers, M.J., Hardenberg, G., Wegmann, F., Zuijdgeest, D., de Wilde, A.H., Koornneef, A., Verwilligen, A., 2020. Ad26 vector-based COVID-19 vaccine encoding a prefusion-stabilized SARS-CoV-2 spike immunogen induces potent humoral and cellular immune responses. NPJ Vaccines 5, 91.

Capone, S., Raggioli, A., Gentile, M., Battella, S., Lahm, A., Sommella, A., Contino, A.M., Urbanowicz, R.A., Scala, R., Barra, F., 2021. Immunogenicity of a new gorilla adenovirus vaccine candidate for COVID-19. Mol. Ther. 29, 2412–2423.

Elkashif, A., Alhashimi, M., Sayedahmed, E.E., Sambhara, S., Mittal, S.K., 2021. Adenoviral vector-based platforms for developing effective vaccines to combat respiratory viral infections. Clin. Transl. Immunology 10, e1345.

Ge, J., Wang, R., Ju, B., Zhang, Q., Sun, J., Chen, P., Zhang, S., Tian, Y., Shan, S., Cheng, L., 2021. Antibody neutralization of SARS-CoV-2 through ACE2 receptor mimicry. Nat. Commun. 12, 250.

Hassan, A.O., Case, J.B., Winkler, E.S., Thackray, L.B., Kafai, N.M., Bailey, A.L., McCune, B.T., Fox, J.M., Chen, R.E., Alsoussi, W.B., 2020. A SARS-CoV-2 infection model in mice demonstrates protection by neutralizing antibodies. Cell 182, 744–753.

Heath, P.T., Galiza, E.P., Baxter, D.N., Boffito, M., Browne, D., Burns, F., Chadwick, D.R., Clark, R., Cosgrove, C., Galloway, J., 2021. Safety and efficacy of NVX-CoV2373 COVID-19 vaccine. N. Engl. J. Med. 385, 1172–1183.

Huang, Q., Ji, K., Tian, S., Wang, F., Huang, B., Tong, Z., Tan, S., Hao, J., Wang, Q., Tan, W., 2021. A single-dose mRNA vaccine provides a long-term protection for hACE2 transgenic mice from SARS-CoV-2. Nat. Commun. 12, 776.

JHU, 2021. COVID-19 Dashboard by the Center for Systems Science and Engineering (CSSE) at Johns Hopkins University (JHU). https://coronavirus.jhu.edu/map.html.

Keech, C., Albert, G., Cho, I., Robertson, A., Reed, P., Neal, S., Plested, J.S., Zhu, M., Cloney-Clark, S., Zhou, H., 2020. Phase 1–2 trial of a SARS-CoV-2 recombinant spike protein nanoparticle vaccine. N. Engl. J. Med. 383, 2320–2332.

Kerstetter, L.J., Buckley, S., Bliss, C.M., Coughlan, L., 2021. Adenoviral vectors as vaccines for emerging avian influenza viruses. Front. Immunol. 11, 607333.

Khoury, D.S., Cromer, D., Reynaldi, A., Schlub, T.E., Wheatley, A.K., Juno, J.A., Subbarao, K., Kent, S.J., Triccas, J.A., Davenport, M.P., 2021. Neutralizing antibody levels are highly predictive of immune protection from symptomatic SARS-CoV-2 infection. Nat. Med. 27, 1205–1211.

Laczkó, D., Hogan, M.J., Toulmin, S.A., Hicks, P., Lederer, K., Gaudette, B.T., Castaño, D., Amanat, F., Muramatsu, H., Oguin III, T.H., Ojha, A., Zhang, L., Mu, Z., Parks, R., Manzoni, T.B., Roper, B., Strohmeier, S., Tombácz, I., Arwood, L., Nachbagauer, R., Karikó, K., Greenhouse, J., Pessaint, P., Porto, M., Putman-Taylor, T., Strasbaugh, A., Campbell, T., Lin, P.J.C., Tam, Y.K., Sempowski, G.D., Farzan, M., Choe, H., Saunders, K.O., Haynes, B.F., Andersen, H., Eisenlohr, L.C., Weissman, D., Krammer, F., Bates, P., Allman, D., Locci, M., Pardi, N., 2020. A single immunization with nucleoside-modified mRNA vaccines elicits strong cellular and humoral immune responses against SARS-CoV-2 in mice. Immunity 53, 724–732.

Li, W., Chen, C., Drelich, A., Martinez, D.R., Gralinski, L.E., Sun, Z., Schäfer, A., Kulkarni, S.S., Liu, X., Leist, S.R., 2020. Rapid identification of a human antibody with high prophylactic and therapeutic efficacy in three animal models of SARS-CoV-2 infection. Proc. Natl. Acad. Sci. U.S.A. 117, 29832–29838.

Li, K., Meyerholz, D.K., Bartlett, J.A., McCray Jr., P.B., 2021a. The TMPRSS2 inhibitor nafamostat reduces SARS-CoV-2 pulmonary infection in mouse models of COVID-19. mBio 12, e0097021.

Li, M., Guo, J., Lu, S., Zhou, R., Shi, H., Shi, X., Cheng, L., Liang, Q., Liu, H., Wang, P., Wang, N., Wang, Y., Fu, L., Xing, M., Wang, R., Ju, B., Liu, L., Lau, S.-Y., Jia, W., Tong, X., Yuan, L., Guo, Y., Qi, H., Zhang, Q., Huang, Z., Chen, H., Zhang, Z., Chen, Z., Peng, X., Zhou, D., Zhang, L., 2021b. Single-dose immunization with a chimpanzee adenovirus-based vaccine induces sustained and protective immunity against SARS-CoV-2 infection. Front. Immunol. 12, 697074.

Liu, Q., Xiong, Q., Mei, F., Ma, C., Zhang, Z., Hu, B., Xu, J., Jiang, Y., Zhan, F., Zhou, S., Tao, L., Chen, X., Guo, M., Wang, X., Fang, Y., Shen, S., Liu, Y., Liu, F., Zhou, L., Xu, K., Ke, C., Deng, F., Cai, K., Yan, H., Chen, Y., Lan, K., 2021. Antibody neutralization to SARS-CoV-2 and variants after one year in Wuhan, China. Innovation 3, 100181.

Logunov, D.Y., Dolzhikova, I.V., Shcheblyakov, D.V., Tukhvatulin, A.I., Zubkova, O.V., Dzharullaeva, A.S., Kovyrshina, A.V., Lubenets, N.L., Grousova, D.M., Erokhova, A.S., 2021. Safety and efficacy of an rAd26 and rAd5 vector-based heterologous prime-boost COVID-19 vaccine: an interim analysis of a randomised controlled phase 3 trial in Russia. Lancet 397, 671–681.

Ma, X., Zou, F., Yu, F., Li, R., Yuan, Y., Zhang, Y., Zhang, X., Deng, J., Chen, T., Song, Z., 2020. Nanoparticle vaccines based on the receptor binding domain (RBD) and heptad repeat (HR) of SARS-CoV-2 elicit robust protective immune responses. Immunity 53, 1315–1330.e9.

McMahan, K., Yu, J., Mercado, N.B., Loos, C., Tostanoski, L.H., Chandrashekar, A., Liu, J., Peter, L., Atyeo, C., Zhu, A., Bondzie, E.A., Dagotto, G., Gebre, M.S., Jacob-Dolan, C., Li, Z., Nampanya, F., Patel, S., Pessaint, L., Ry, A.V., Blade, K., Yalley-Ogunro, J., Cabus, M., Brown, R., Cook, A., Teow, E., Andersen, H., Lewis, M.J., Lauffenburger, D.A., Alter, G., Barouch, D.H., 2021. Correlates of protection against SARS-CoV-2 in rhesus macaques. Nature 590, 630–634.

Mendonça, S.A., Lorincz, R., Boucher, P., Curiel, D.T., 2021. Adenoviral vector vaccine platforms in the SARS-CoV-2 pandemic. NPJ Vaccines 6, 97.

Ong, S.W.X., Tan, Y.K., Chia, P.Y., Lee, T.H., Ng, O.T., Wong, M.S.Y., Marimuthu, K., 2020. Air, surface environmental, and personal protective equipment contamination by severe acute respiratory syndrome coronavirus 2 (SARS-CoV-2) from a symptomatic patient. JAMA 323, 1610–1612.

Palacios, R., Patiño, E.G., de Oliveira Piorelli, R., Conde, M.T.R.P., Batista, A.P., Zeng, G., Xin, Q., Kallas, E.G., Flores, J., Ockenhouse, C.F., 2020. Double-blind, randomized, placebo-controlled phase iii clinical trial to evaluate the efficacy and safety of treating healthcare professionals with the adsorbed COVID-19 (inactivated) vaccine manufactured by Sinovac-PROFISCOV: a structured summary of a study protocol for a randomised controlled trial. Trials 21, 853.

Polack, F.P., Thomas, S.J., Kitchin, N., Absalon, J., Gurtman, A., Lockhart, S., Perez, J.L., Marc, G.P., Moreira, E.D., Zerbini, C., Bailey, R., Swanson, K.A., Roychoudhury, S., Koury, K., Li, P., Kalina, W.V., Cooper D., Jr, R.W.F., Hammitt, L.L., Türeci, Ö., Nell, H., Schaefer, A., Ünal, S., Tresnan, D.B., Mather, S., Dormitzer, P.R., Şahin, U., Jansen, K.U., Gruber, W.C., C4591001 Clinical Trial Group, 2020. Safety and efficacy of the BNT162b2 mRNA Covid-19 vaccine. N. Engl. J. Med. 383, 2603–2615.

Rathnasinghe, R., Strohmeier, S., Amanat, F., Gillespie, V.L., Krammer, F., García-Sastre, A., Coughlan, L., Schotsaert, M., Uccellini, M.B., 2020. Comparison of transgenic and adenovirus hACE2 mouse models for SARS-CoV-2 infection. Emerg. Microbes. Infect. 9, 2433–2445.

Scheuch, G., 2020. Breathing is enough: for the spread of influenza virus and SARS-CoV-2 by breathing only. J. Aerosol. Med. Pulm. Drug. Deliv. 33, 230–234.

Sun, J., Zhuang, Z., Zheng, J., Li, K., Wong, R.L.-Y., Liu, D., Huang, J., He, J., Zhu, A., Zhao, J., Li, X., Xi, Y., Chen, R., Alshukairi, A.N., Chen, Z., Zhang, Z., Chen, C., Huang, X., Li, F., Lai, X., Chen, D., Wen, L., Zhuo, J., Zhang, Y., Wang, Y., Huang, S., Dai, J., Shi, Y., Zheng, K., Leidinger, M.R., Chen, J., Li, Y., Zhong, N., Meyerholz, D.K., Jr, P.B.M., Perlman, S., Zhao, J., 2020a. Generation of a broadly useful model for COVID-19 pathogenesis, vaccination, and treatment. Cell 182, 734–743e5.

Sun, S.-H., Chen, Q., Gu, H.-J., Yang, G., Wang, Y.-X., Huang, X.-Y., Liu, S.-S., Zhang, N.-N., Li, X.-F., Xiong, R., 2020b. A mouse model of SARS-CoV-2 infection and pathogenesis. Cell Host Microbe 28, 124–133.e4.

Tostanoski, L.H., Wegmann, F., Martinot, A.J., Loos, C., McMahan, K., Mercado, N.B., Yu, J., Chan, C.N., Bondoc, S., Starke, C.E., Nekorchuk, M., Busman-Sahay, K., Piedra-Mora, C., Wrijil, L.M., Ducat, S., Custers, J., Atyeo, C., Fischinger, S., Burke, J.S., Feldman, J., Hauser, B.M., Caradonna, T.M., Bondzie, E.A., Dagotto, G., Gebre, M.S., Jacob-Dolan, C., Lin, Z., Mahrokhian, S.H., Nampanya, F., Nityanandam, R., Pessaint, L., Porto, M., Ali, V., Benetiene, D., Tevi, K., Andersen, H., Lewis, M.G., Schmidt, A.G., Lauffenburger, D.A., Alter, G., Estes, J.D., Schuitemaker, H., Zahn, R., Barouch, D.H., 2020. Ad26 vaccine protects against SARS-CoV-2 severe clinical disease in hamsters. Nat. Med. 26, 1694–1700.

van Doremalen, N., Lambe, T., Spencer, A., Belij-Rammerstorfer, S., Purushotham, J.N., Port, J.R., Avanzato, V.A., Bushmaker, T., Flaxman, A., Ulaszewska, M., Feldmann, F., Allen, E.R., Sharpe, H., Schulz, J., Holbrook, M., Okumura, A., Meade-White, K., Pérez-Pérez, L., Edwards, N.J., Wright, D., Bissett, C., Gilbride, C., Williamson, B.N., Rosenke, R., Long, D., Ishwarbhai, A., Kailath, R., Rose, L., Morris, S., Powers, C., Lovaglio, J., Hanley, P.W., Scott, D., Saturday, G., Wit, E.d., Gilbert, S.C., Munster, V.J., 2020. ChAdOx1 nCoV-19 vaccine prevents SARS-CoV-2 pneumonia in rhesus macaques. Nature 586, 578–582.

Wang, H., Zhang, Y., Huang, B., Deng, W., Quan, Y., Wang, W., Xu, W., Zhao, Y., Li, N., Zhang, J., Liang, H., Bao, L., Xu, Y., Ding, L., Zhou, W., Gao, H., Liu, J., Niu, P., Zhao, L., Zhen, W., Fu, H., Yu, S., Zhang, Z., Xu, G., Li, C., Lou, Z., Xu, M., Qin, C., Wu, G., Gao, G.F., Tan, W., Yang, X., 2020. Development of an inactivated vaccine candidate, BBIBP-CorV, with potent protection against SARS-CoV-2. Cell 182, 713–721.e9.

WHO, 2021a. Prequalification of Medical Products (IVDs, Medicines, Vaccines and Immunization Devices, Vector Control). https://extranet.who.int/pqweb/vaccines/vaccinescovid-19-vaccine-eul-issued.

WHO, 2021b. COVID-19 vaccine tracker and landscape. https://www.who.int/publications/m/item/draft-landscape-of-covid-19-candidate-vaccines.

Xu, K., An, Y., Li, Q., Huang, W., Han, Y., Zheng, T., Fang, F., Liu, H., Liu, C., Gao, P., Xu, S., Liu, X., Zhang, R., Zhao, X., Liu, W.J., Bi, Y., Wang, Y., Zhou, D., Wang, Q., Hou, W., Xia, Q., Gao, G.F., Dai, L., 2021. Recombinant chimpanzee adenovirus AdC7 expressing dimeric tandem-repeat spike protein RBD protects mice against COVID-19. Emerg. Microbes. Infect. 10, 1574–1588.

Yang, J., Wang, W., Chen, Z., Lu, S., Yang, F., Bi, Z., Bao, L., Mo, F., Li, X., Huang, Y., Hong, W., Yang, Y., Zhao, Y., Ye, F., Lin, S., Deng, W., Chen, H., Lei, H., Zhang, Z., Luo, M., Gao, H., Zheng, Y., Gong, Y., Jiang, X., Xu, Y., Lv, Q., Li, D., Wang, M., Li, F., Wang, S., Wang, G., Yu, P., Qu, Y., Yang, L., Deng, H., Tong, A., Li, J., Wang, Z., Yang, J., Shen, G., Zhao, Li, Y., Luo, J., Liu, H., Yu, W., Yang, M., Xu, J., Wang, J., Li, H., Wang, H., Kuang, D., Lin, P., Hu, Z., Guo, W., Cheng, W., He, Y., Song, X., Chen, C., Xue, Z., Yao, S., Chen, Lu., Ma, X., Chen, S., Gou, M., Huang, W., Wang, Y., Fan, C., Tian, Z., Shi, M., Wang, F.-S., Dai, L., Wu, M., Li, G., Wang, G., Peng, Y., Qian, Z., Huang, C., Lau, J.Y.-N., Yang, Z., Wei, Y., Cen, X., Peng, X., Qin, C., Zhang, K., Lu, G., Wei, X., 2020. A vaccine targeting the RBD of the S protein of SARS-CoV-2 induces protective immunity. Nature 586, 572–577.

Zhu, F.-C., Li, Y.-H., Guan, X.-H., Hou, L.-H., Wang, W.-J., Li, J.-X., Wu, S.-P., Wang, B.-S., Wang, Z., Wang, L., Jia, S.-Y., Jiang, H.-D., Wang, L., Jiang, T., Hu, Y., Gou, J.-B., Xu, S.-B., Xu, J.-J., Wang, X.-W., Wang, W., Chen, W., 2020a. Safety, tolerability, and immunogenicity of a recombinant adenovirus type-5 vectored COVID-19 vaccine: a dose-escalation, open-label, non-randomised, first-in-human trial. Lancet 395, 1845–1854.

Zhu, N., Zhang, D., Wang, W., Li, X., Yang, B., Song, J., Zhao, X., Huang, B., Shi, W., Lu, R., Niu, P., Zhan, F., Ma, X., Wang, D., Xu, W., Wu, G., Gao, G.F., Tan, W., China Novel Coronavirus Investigating and Research Team, 2020b. A novel coronavirus from patients with pneumonia in China, 2019. N. Engl. J. Med. 382, 727–733.